Acta Neuropathol (2011) 121:487–498
DOI 10.1007/s00401-010-0788-5

ORIGINAL PAPER

Modulation of lipid peroxidation and mitochondrial function improves neuropathology in Huntington's disease mice

Junghee Lee · Bela Kosaras · Steve J. Del Signore · Kerry Cormier · Ann McKee · Rajiv R. Ratan · Neil W. Kowall · Hoon Ryu

Received: 23 May 2010 / Revised: 21 November 2010 / Accepted: 2 December 2010 / Published online: 16 December 2010

Abstract Huntington's disease (HD) is an autosomal dominant neurodegenerative disorder. Oxidative damage has been associated with pathological neuronal loss in HD. The therapeutic modulation of oxidative stress and mitochondrial function using low molecular weight compounds may be an important strategy for delaying the onset and slowing the progression of HD. In the present study, we found a marked increase of 4-hydroxy-2-nonenal (4-HNE) adducts, a lipid peroxidation marker, in the caudate and putamen of HD brains and in the striatum of HD mice. Notably, 4-HNE immunoreactivity was colocalized with mutant huntingtin inclusions in the striatal neurons of R6/2 HD mice. Administration of nordihydroguaiaretic acid (NDGA), an antioxidant that functions by inhibiting lipid peroxidation, markedly reduced 4-HNE adduct formation in the nuclear inclusions of R6/2 striatal neurons. NDGA also protected cultured neurons against oxidative stress-induced cell death by improving ATP generation and mitochondrial morphology and function. In addition, NDGA restored mitochondrial membrane potential, mitochondrial structure, and synapse structure in the striatum of R6/2 mice and increased their lifespan. The present findings suggest that further therapeutic studies using NDGA are warranted in HD and other neurodegenerative diseases characterized by increased oxidative stress and altered mitochondrial function.

Keywords Huntington's disease · Mitochondria · Lipid peroxidation · 4-Hydroxy-2-nonenal (4-HNE) · Neuronal survival

Electronic supplementary material The online version of this article (doi:10.1007/s00401-010-0788-5) contains supplementary material, which is available to authorized users.

J. Lee · S. J. Del Signore · K. Cormier · A. McKee · N. W. Kowall · H. Ryu
Department of Neurology and Pathology, Boston University School of Medicine, Boston, MA 02118, USA

J. Lee · N. W. Kowall · H. Ryu (✉)
VA Boston Healthcare System, Building 1A, Rm 109, Boston, MA 02130, USA
e-mail: hoonryu@bu.edu

B. Kosaras
Department of Neurology, Beth Israel Deaconess Medical Center and Harvard Medical School, Boston, MA 02115, USA

S. J. Del Signore · K. Cormier · A. McKee
Bedford VA Medical Center, Bedford, MA 01730, USA

R. R. Ratan
Department of Neurology, Weill Medical College of Cornell University, Burke-Cornell Medical Research Institute, White Plains, NY 10605, USA

Introduction

Huntington's disease (HD) is a fatal autosomal dominant neurodegenerative disease of midlife onset caused by an expanded DNA segment containing a polymorphic trinucleotide CAG repeat that encodes the protein huntingtin (Htt) [14, 15]. The Htt protein is widely and heterogeneously expressed in neurons throughout the brain. There is increasing evidence suggesting that mtHtt and its proteolytic fragments may participate in pathologic protein–protein interactions, leading to altered genetic and molecular messages that result in neuronal dysfunction [4, 9, 44]. A direct pathway linking the genetic mutation to neuronal degeneration, however, has not been established.

Impaired energy metabolism due to mitochondrial dysfunction and oxidative damage occur in HD, but it is not clear whether neuronal injury is a cause or result of oxidative damage [1, 3]. It is noteworthy that lymphoblasts from HD patients manifest abnormal mitochondrial membrane depolarization suggesting that mitochondrial dysfunction in the HD brain is not secondary to neuropathological alterations [30, 37]. Mitochondrial dysfunction may be disease-specific because lymphoblasts from the patients with spinocerebellar ataxia type 1 (SCA1), another neurodegenerative disorder caused by an expanded poly Q in the gene *ataxin-1*, do not show altered mitochondrial membrane depolarization [37]. Furthermore, oxidative damage affects mitochondrial DNA in the parietal cortex as well as nuclear DNA in the caudate nucleus in HD [6] confirming the notion that oxidative stress is a fundamental aspect of HD pathogenesis [45]. Because of this, therapeutic modulation of oxidative stress and mitochondrial function using small compounds may be an important strategy for slowing the onset and the progression of HD [4, 35].

Polyunsaturated fatty acids within the cellular membrane are among the primary targets of free radicals. 4-Hydroxy-2-nonenal (4-HNE), a major lipid peroxidation product of $n - 6$ polyunsaturated fatty acids, interferes with nucleophilic and signaling molecules that regulate a wide range of cellular processes including proliferation, differentiation, and apoptosis [7]. 4-HNE induces neuronal microtubule dysfunction and inhibits neurite outgrowth and is elevated in the brain and plasma of Alzheimer's patients [21–24]. 4-HNE deposition has also been found in other neurodegenerative diseases, including amyotrophic lateral sclerosis, myotonic dystrophy, and Parkinson's disease [5, 12, 29], but 4-HNE adducts have not been previously investigated in HD.

In this study, we examined the level of 4-HNE adducts in human and murine HD brains. We also evaluated the therapeutic effects of a phytoestrogen, nordihydroguaiaretic acid (NDGA), on oxidative stress and mitochondrial function in an animal model of HD.

Materials and methods

Animals and therapeutic intervention

Male transgenic HD mice (R6/2 strain) [20] were obtained from The Jackson Laboratory (Bar Harbor, ME, USA) and maintained as a colony at the Bedford Veterans Medical Center. CAG140 mice and N171-82Q mice were obtained from Dr. Levine and Dr. Borchelt's laboratory, respectively [17, 39]. All mice were handled under the same conditions by one investigator as described previously [8, 36]. All mice were weighed at 20 days of age and equally distributed according to weight and percentage within each cohort ($n = 10$). NDGA (12 mg/kg/day; Calbiochem) was administered by intraperitoneal (i.p.) injection at 30 days of age. NDGA was injected five times a week. Control groups were treated with saline injection. For all groups, body weight was measured and recorded twice weekly at the same time and day. For the neuropathological and the biochemical analysis, R6/2, N171-82Q, and CAG140 mice were euthanized at 90 days (3 months), 180 days (6 months), and 240 days (8 months) of age, respectively. A limited number of deaths occurred overnight and were recorded the following morning. All animal experiments were performed in accordance with the National Institutes of Health *Guide for the Care and Use of Laboratory Animals* and were approved by both the Veterans Administration and Boston University Animal Care Committees.

Human tissue samples

Samples of striatum and the superior frontal cortex were pathologically verified and graded according to neuropathological criteria as described previously [36, 46]. The information on human brain samples was shown in Online Resource 1.

Primary cortical neuron culture

The primary neurons were obtained from the cerebral cortex of fetal Sprague–Dawley rats [embryonic day 17 (E17)] and B6CBA mice (E15) as described previously [32, 33]. All experiments were initiated 24–72 h or 2 weeks in vitro culture after plating. Neurons were either stimulated with indicated agonists and antagonist or treated with the same volume of the appropriated diluents for the indicated periods of time. Neuronal cell viability was assessed by phase-contrast microscopy, MTT, and TUNEL assay [34].

Intracellular ATP measurement

Primary neurons were treated NDGA for 24 h. The cell lysates were prepared for the measurement of ATP using a bioluminescence detection kit for ATP (Promega, Madison, WI, USA).

Western blot analysis

For the measurement of protein level by Western blot analysis, the minced brains from WT and R6/2 mice were homogenized with 15 strokes (Power Gen 125, Fisher Scientific, Pittsburgh, PA, USA) in an ice-cold cell extraction buffer containing 50 mM Tris–HCl, pH 7.4, 150 mM NaCl, 2 mM EDTA, 1% Triton X-100, 1 mM

(PMSF), 10 μg/ml leupeptin, 1 mM pepstatin, 1 mM *N*-ethylmaleimide, 2 mM Na_3VO_4, 20 mM sodium pyrophosphate, and 50 mM NaF [33]. The supernatants were carefully removed, and the protein concentration was quantified by Bradford method. Lysates were mixed with 2× or 5× boiling Laemmli's buffer (1× is 100 mM Tris–HCl, pH 6.8, 4% SDS, 200 mM dithiothreitol, 20% glycerol, 2% SDS, 0.2% bromophenol blue, 10 μg/ml aprotinin, 10 μg/ml leupeptin). The samples were then boiled for 10 min at 100°C and spun at 15,000 rpm for 10 s. Typically, about 30 μg of protein was electrophoresed on 10% SDS-polyacrylamide gel and transferred to nitrocellulose membrane. Membranes were blocked in 5% skim milk in TBST (Tris, pH 7.4; 150 mM NaCl; 0.05% Tween 20) for 30 min at room temperature. Blots were then probed with primary antibodies overnight at 4°C followed by incubation with anti-rabbit or anti-mouse IgG, conjugated with horseradish peroxidase (Bio-Rad, Hercules, CA, USA) for 1 h. Signals were detected by using the ECL system (Amersham Corp., Arlington Heights, IL, USA).

Neuropathology and confocal microscopy

Serial-cut coronal tissue sections from the rostral segment of the neostriatum at the level of the anterior commissure (interaural 5.34 mm, bregma 1.54 mm to interaural 3.7 mm, bregma −0.10 mm) were used for the neuropathological analysis [8, 36]. Serially cut tissue sections were stained for Nissl substance, and the neuronal sizes were analyzed by NIH ImageJ program. Indirect labeling methods were used to determine the levels of 4-HNE (Chemicon, Temecular, CA, USA) (1:200), MDA (Chemicon) (1:200), mtHtt (EM48 monoclonal antibody) (Chemicon) (1:1,000), cytochrome *c* (Santa Cruz Biotech) (1:200), and βIII tubulin (Sigma) (1:500 dilution). Fixed cells and tissue sections were incubated with blocking solution containing 0.3% Triton X-100, 5% bovine serum albumin, and 3% goat serum for 1 h, followed by incubation with primary antibodies overnight at 4°C. After three washes with PBS, the specimens were incubated for 1 h with FITC and Cy3-conjugated secondary antibodies (1:200 dilution). The nucleus was counter stained with 4′,6-diamidino-2-phenylindole (DAPI). All antibodies were diluted in PBS. The slides were washed three times with PBS and mounted with fluorochrome mounting solution (Vector Laboratories). Images were analyzed using a spinning disk confocal microscope (Olympus DSU, Tokyo, Japan). Deconvolution and three-dimensional construction of the confocal image were performed by AQI-X-COMBO-CWF program (Media cybernetics Inc., Bethesda, MD, USA). Isosurface image was reconstructed after a deconvolution of the confocal image. "Isosurfaces" are a graphical rendering technique available on the more powerful computer visualization programs, which create 2D contours in 3D space by interpolating between stacked sequential images, such as the 2D cellular maps that comprise a cross-section of the 3D data volume. Typically, we looked at a series of 40 confocal layers representing fluorescence data from the substantia nigra neuron and then developed an abstract image which provided the details seen in this image. The quantitative assessment of the image was measured by AQI-X-COMBO-CWF and NIH ImageJ software. Control experiments were performed either in the absence of primary antibody or in the presence of blocking peptide.

Transmission electron microscopy (TEM)

The primary cultured neurons and brain samples were fixed for 1 h in a mixture of 2% glutaraldehyde, 0.2% freshly prepared tannic acid, and 0.1 M sodium cacodylate (pH 7.4). After washing in cacodylate, they were postfixed in 0.5% OsO_4 and embedded in Durcupan (Fluka, Switzerland). The sections were contrasted with uranyl acetate and lead citrate and examined in a Jeol CX 100 electron microscope.

Statistical analysis

The data are presented as the mean ± SEM. Data analysis was performed by Student *t* test and one-way ANOVA followed by Fisher's protected least significant difference test using StatView 4 (Abacus Concepts, Berkeley, CA, USA). Survival data were analyzed by Kaplan–Meier survival curves. Differences were considered statistically significant when $P < 0.05$.

Results

Increased 4-HNE adducts in the striatum of human HD and animal models of HD

The 4-HNE is a major membrane lipid peroxidation product. While markers of oxidative damage to DNA and proteins have been studied in HD, there has been no such research using 4-HNE. Our aim was to determine the level of 4-HNE in human HD and murine HD brain tissue sections using immunocytochemistry and confocal microscopy. Immunoreactivity of 4-HNE adducts, a lipid peroxidation marker, was markedly increased in the caudate and putamen of the human HD brain compared to the control brain that displayed weak immunoreactivity of 4-HNE adducts (Fig. 1a, b). The information on human brain samples was shown in Online Resource 1. Densitometric analysis by NIH ImageJ showed that the 4-HNE levels are significantly increased both in

caudate and putamen of HD brains in comparison to the control brains ($P < 0.01$, $df = 8$) (Fig. 1c). In addition, we quantified the amount of lipid peroxidation (4-HNE plus MDA) in human samples using a colorimetric microplate assay. Concurrent with the immunohistochemistry data, the total level of lipid peroxidation was significantly elevated in HD brains (2.64 ± 0.20 μM) than in controls (2.13 ± 0.12 μM) ($P < 0.05$, $df = 8$) (Online Resource 2). Otherwise, immunoreactivity of 4-HNE adducts was notably elevated in the nucleus striatal neurons of the N171-82Q HD mouse at 6 months of age (Fig. 2a, b) and in striatal neurons of the CAG140 knock-in HD mouse at 8 months of age (Fig. 2c, d), respectively ($P < 0.05$, $F = 8$). Interestingly, the immunoreactivity of 4-HNE adducts was found in nuclei along with the immunoreactivity of mtHtt (Fig. 2c). We found that oxidative stress increases the cellular immunoreactivity of 4-HNE in a cell line model of HD (Tet-mtHtt-Q103-EGFP cells) (Online Resource 3). Tet-mtHtt Q103-EGFP SH-SY5Y cells were induced with 3 μM of doxycycline for the expression of mtHtt for 48 h. The basal immunoreactivity of 4-HNE adducts was increased by mtHtt induction. Moreover, the level of 4-HNE adducts and aggregates were enhanced when cells were exposed to oxidative stress (10 μM of H_2O_2 for 12 h).

NDGA protects neurons against oxidative stress-induced cell death via mitochondria-dependent pathway

To determine the neuroprotective effect of NDGA, primary neurons were exposed to buthionine sulfoximine (BSO) to induce oxidative stress by glutathione depletion through an inhibition of γ-glutamylcysteine synthetase. NDGA (<10 μM) prevented BSO-induced neuronal death in a concentration-dependent manner (Online Resource 4). However, a higher dose (>10 μM) of NDGA showed no additional protective effect against oxidative stress. Glutamate-induced cell death, which is accompanied by an accumulation of reactive oxygen species (ROS), is a major contributor to pathological cell death within the nervous system. Selective striatal degeneration is mimicked by administration of excitotoxins into the striatum [4]. Thus, glutamate-induced excitotoxicity is closely linked to the oxidative stress in HD. In order to confirm the protective role of NDGA against excitotoxicity, we further investigated the effect of NDGA on the glutamate-induced neuronal cytotoxicity and the ultrastructural morphology of mitochondria using a cytochrome *c* antibody and the MitoTracker probe (CMXRos). The mitochondria were double labeled in the presence or absence of glutamate and NDGA. Control cells showed intact mitochondrial cytochrome *c* staining (green) and CMXRos (red) (Fig. 3a). The fluorescence-staining pattern of active mitochondria in

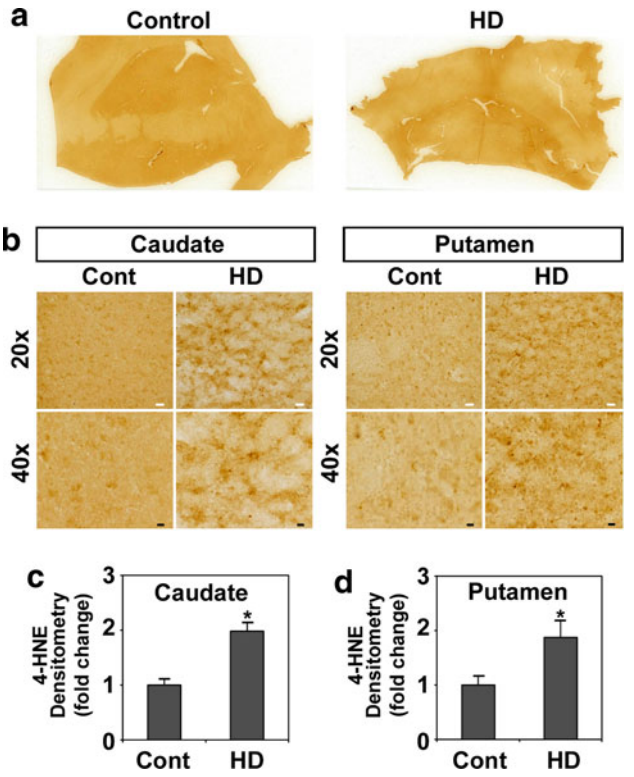

Fig. 1 4-HNE, a lipid peroxidation marker, is increased in Huntington's disease (HD). **a** Immunohistochemistry of 4-HNE adducts in control and human HD brain (grade 3). **b** Immunoreactivity of 4-HNE is increased in caudate and putamen of human HD. **c** and **d** Densitometry shows that the levels of 4-HNE are increased both in caudate and putamen of HD brains ($n = 5$) in comparison to the control brains ($n = 5$). *Scale bars*: *white* 30 μm; *black* 10 μm. Data were analyzed by Student *t* test. *Significantly different from control at $P < 0.05$

control cells was concentrated in the peri-nuclear region. In the presence of glutamate for 18 h, cortical neurons revealed loss of mitochondrial cytochrome *c*, mitochondrial membrane potential, and the loss of mitochondrial fluorescence (Fig. 3a). The change of mitochondrial membrane potential by MitoTracker probe was further analyzed by NIH ImageJ (Online Resource 5). NDGA treatment not only restored the mitochondrial membrane potential, but also inhibited the release of cytochrome *c* to the cytosolic fraction. This is a process that occurs in glutamate-treated cortical neurons prior to cell death (Fig. 3b). NDGA also blocked the cleavage of pro-caspase-9 (cas-9) to active caspase-9 (Fig. 3c). NDGA (1 μM) was neither cytotoxic nor did it compromise the mitochondrial membrane potential (Fig. 3a). These results suggest that the protective role of NDGA against oxidative stress is upstream of a mitochondria-dependent death pathway in neurons. Glutamate treatment disrupted the mitochondrial membrane and cristae structure in comparison to normal mitochondria (Fig. 3d). NDGA prevented the structural damage of mitochondria in response to glutamate (Fig. 3d).

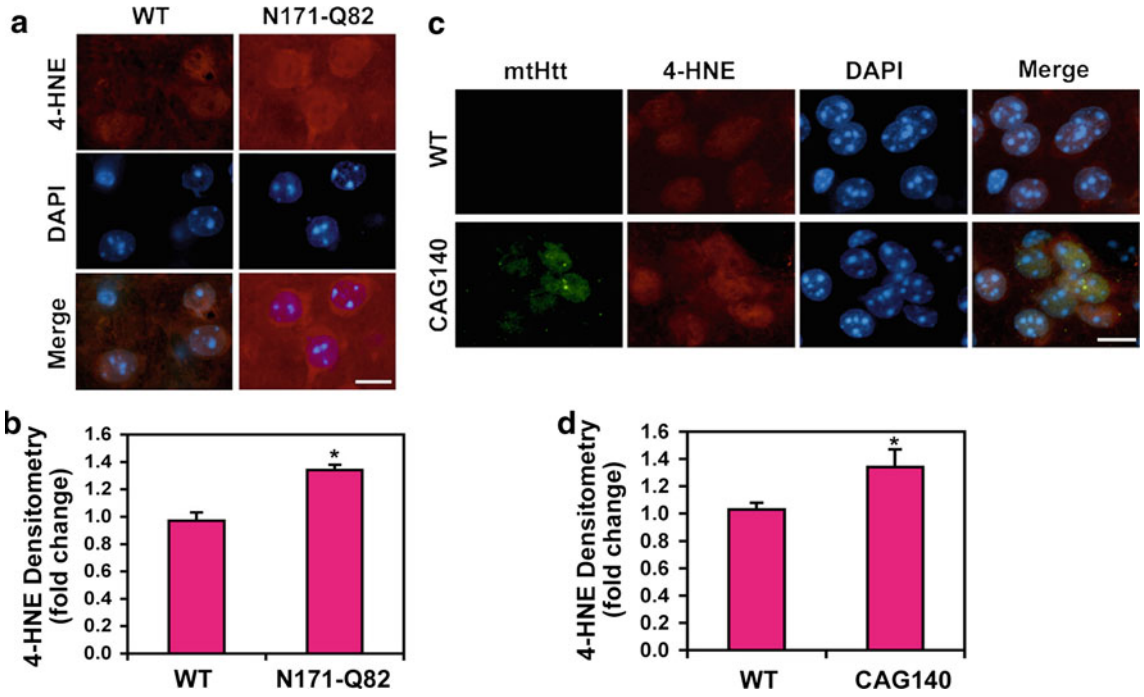

Fig. 2 4-HNE is increased in animal models of HD. **a** Immunoreactivity of 4-HNE adducts is elevated in striatal neurons of N171-82Q HD mice. **b** Immunoreactivity of 4-HNE adducts is increased in striatal neurons of CAG140 knock-in HD mice. Note the elevation of nuclear immunoreactivity of 4-HNE in both N171-82Q and CAG140 knock-in mouse. **c** and **d** Densitometry shows that 4-HNE adducts are increased in N171-82Q and CAG140 knock-in mice in comparison to WT mice. *Scale bars*: *white* 10 μm. Data were analyzed by Student *t* test. *Significantly different from control at $P < 0.05$

These electron microscopic data further support that NDGA effectively prevents neuronal damage upstream of the mitochondria-dependent pathway. Recently, the proposition that defects in mitochondrial energy metabolism underlie the pathogenesis of neuronal loss in neurodegenerative disorders has gained considerable support. To establish a relationship between NDGA and energy metabolism, we measured ATP in primary neuron cultures. Mouse cortico-striatal primary neurons were treated with NDGA for 24 h, and cell lysates were prepared for the measurement of ATP using a bioluminescence detection kit for ATP. NDGA increased the intracellular level of ATP in a dose-dependent manner (Fig. 3e).

NDGA reduces the level of 4-HNE adducts and aggregates of mutant huntingtin (mtHtt) in R6/2 HD mouse

To determine if NDGA would provide therapeutic benefit in a transgenic mouse model of HD, we assessed the relationship of the anti-oxidant effect of NDGA in HD mice through phenotypic observation along with 4-HNE adducts using confocal microscopy (Fig. 4a). NDGA decreased the immunoreactivity of 4-HNE adducts in the striatal neurons of R6/2 mice. NDGA was found to also reduce the particle number of 4-HNE adducts (Fig. 4b). The particle numbers were counted from the images shown in the panel *a* using an image-analyzing program (IP Lab, Scanalytics BD Biosciences-Bioimaging). The density (pixel values) of 4-HNE adducts was reduced by NDGA administration in R6/2 mice as well (Fig. 4c). Furthermore, we found that NDGA reduces mtHtt aggregates in the striatal neurons of R6/2 mice compared to vehicle-treated R6/2 mice (Fig. 4d). Inclusion bodies and aggregates formed by mtHtt (exon1 N-terminal mutant Htt fragment) are known to often correlate with neuronal cytotoxicity, so we also analyzed the density mtHtt aggregates (Fig. 4d), which was determined from the images in panel *d*. NDGA administration decreased the density of mtHtt aggregates in R6/2 mice (Fig. 4e). Western blot analysis was used to detect mtHtt in the detergent soluble fraction (Sol. Frac.) and insoluble fraction (Insol. Frac.) of striatal extracts (Fig. 4f). Our research indicates that NDGA reduces the density level of mtHtt in the insoluble fraction (Fig. 4g).

Colocalization of mtHtt with 4-HNE adducts in nuclear inclusions and its reduction by NDGA

Additionally, we analyzed the effect of NDGA on the intracellular and spatial distributions of 4-HNE adducts in striatal neurons using confocal microscopy and image analysis program (IP Lab, Scanalytics BD Biosciences-

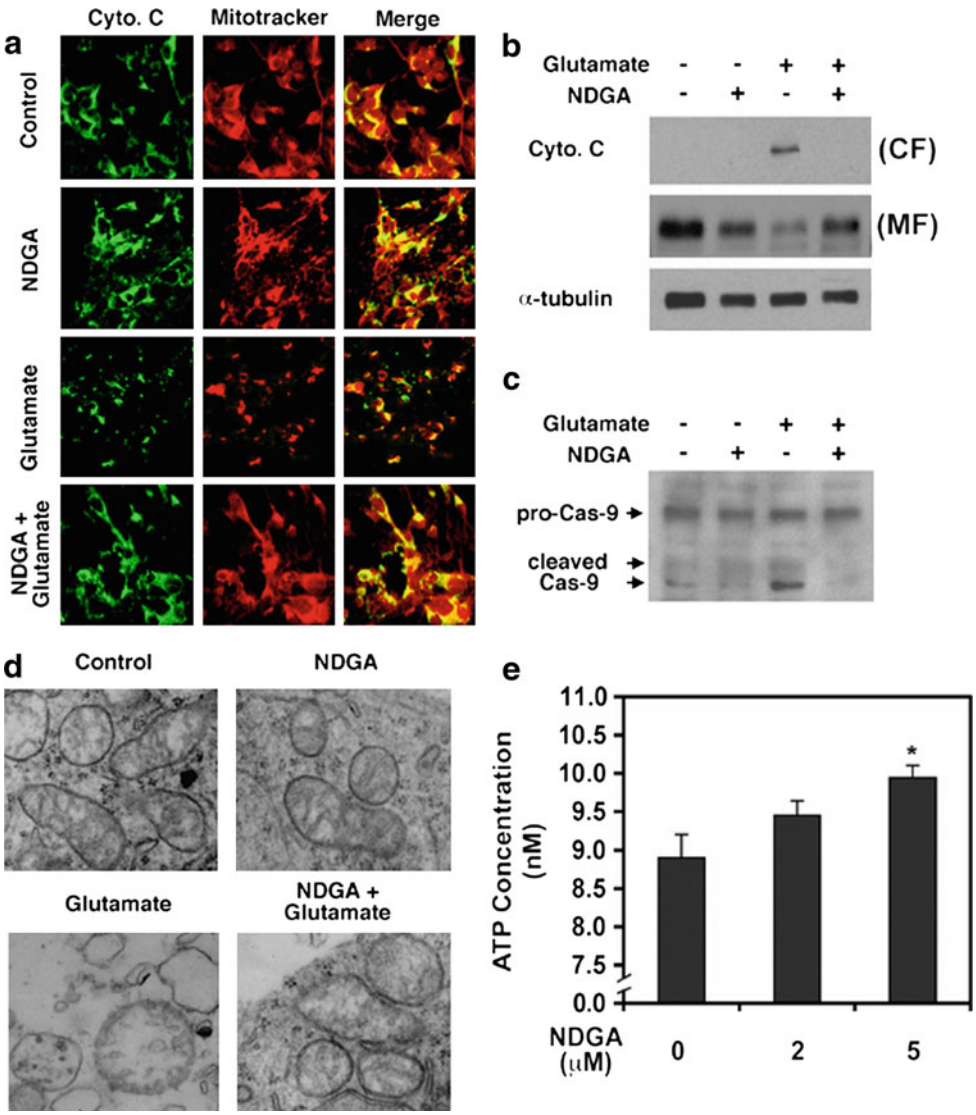

Fig. 3 Norhihydroguaiaretic acid (NDGA), an inhibitor of lipid peroxidation, prevents mitochondrial damage and neuronal death. **a** NDGA protects primary neurons from glutamate-induced mitochondrial damage. Confocal microscopy was performed to determine the level of mitochondrial potential (MitoTracker; CMXRos) and cytochrome *c* (*Cyto. C*) (*green*). Neurons were pretreated with NDGA (1 μM) 1 h before glutamate (100 μM) treatment. **b** Cytochrome *c* release was measured by Western blot analysis in response to glutamate with or without NDGA. NDGA blocks the cytochrome *c* release from mitochondrial fraction (*MF*) to cytosolic fraction (*CF*). **c** NDGA prevents the cleavage of pro-Cas-9 to active Cas-9. **d** NDGA treatment preserves mitochondrial morphology in primary neurons against oxidative stress. **e** NDGA elevates the level of ATP in primary neurons. Data were analyzed by Student *t* test. *Significantly different from zero dosage control at $P < 0.05$

Bioimaging and AQI-X-COMBO-CWF, Media cybernetics Inc. Bethesda, MD, USA). The immunoreactivity of 4-HNE adducts (red color) was distributed in nuclear foci which are spatially colocalized with mtHtt in striatal neurons of the R6/2 mice (Fig. 5). As expected, NDGA decreased the 4-HNE immunoreactivity in neurons of R6/2 mice while the majority of 4-HNE immunoreactivity was spatially merged to the prominent clusters of mtHtt in vehicle-treated R6/2 mice (Fig. 5a). The line measurement for the colocalization spots of 4-HNE and mtHtt showed a marked decrease in the intensity of two molecules in NDGA-administered R6/2 mice compared to vehicle-administered R6/2 mice (Fig. 5b). The administration of NDGA also decreased the Pearson's coefficient for colocalization of 4-HNE with mtHtt in R6/2 mice (Fig. 5c). Isosurface image data of the striatal section, which provided a more powerful computer rendering, was reconstructed after a deconvolution of the confocal image by AQI-X-COMBO-CWF program (Media cybernetics Inc., Bethesda, MD, USA). We studied a series of 40 confocal layers representing fluorescence data from the striatal section and then developed an abstract image which provided the details seen in Fig. 4d. Additionally, ortho-slice images show the colocalization of 4-HNE adducts with mtHtt and its reduction by NDGA.

NDGA improves the membrane potential and the structure of mitochondria and synapse in transgenic HD (R6/2) mice

In addition to in vitro experiments, we studied the intraperitoneal injections of NDGA-improved mitochondrial dysfunction in HD (R6/2) transgenic mice. We assessed the mitochondrial membrane potential in vivo using MitoTracker (CMXRos). CMXRos immunofluorescence was detected in striatal cells of WT and R6/2 mice (Fig. 6a). In

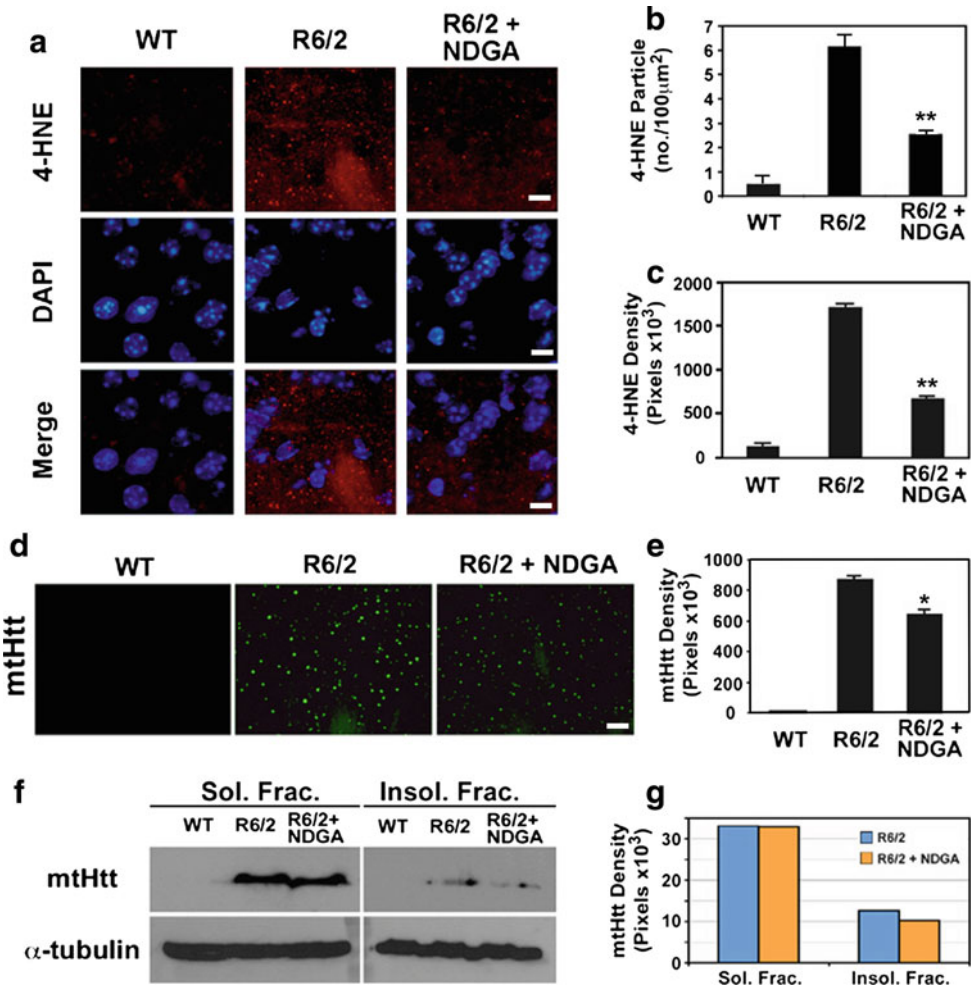

Fig. 4 NDGA reduces the level of 4-HNE adducts and aggregates of mtHtt in R6/2 mice. **a** NDGA decreased the immunoreactivity of 4-HNE adducts in the striatal neurons of R6/2 mice (R6/2 + NDGA) compared to vehicle-treated R6/2 mice (R6/2). *Scale bars*: *white* 10 μm. **b** NDGA reduced the particle number of 4-HNE adducts. The particle numbers were counted from the images shown in **a**. Images taken from three fields were analyzed. **c** The density reduction of 4-HNE adducts by NDGA administration in R6/2 mice. The pixel values were originated and determined from the images in **a**. Particle numbers and density of 4-HNE adducts were determined using an image analyzing program (IP Lab, Scanalytics BD Biosciences-Bioimaging). **d** Confocal microscopy shows that NDGA reduces the mtHtt aggregates in the striatal neurons of R6/2 mice. *Scale bars*: *white* 10 μm. **e** The reduction of mtHtt density by NDGA in R6/2 mice. The pixel values were originated and determined from the images in **d** using an image analyzing program. Images taken from three fields were analyzed. **f** Western blot analysis of mtHtt expression in detergent soluble fraction (*Sol. Frac.*) and insoluble fraction (*Insol. Frac.*). NDGA reduces the level of mtHtt in insoluble fraction. **g** The densitometry of mtHtt adducts by NDGA administration in R6/2 mice. The pixel values were originated and determined from the images in **f**

the R6/2 brain, the immunofluorescence of CMXRos was markedly reduced compared to WT brain. This implies that the mitochondrial dysfunction is a result of lowered mitochondrial membrane potential in R6/2 brains and striatal cells. The NDGA treatment significantly improved the fluorescent intensity of CMXRos in the brain and striatal neurons of R6/2 mice in comparison to the vehicle-treated R6/2 mice (Fig. 6a). The change of mitochondrial membrane potential by MitoTracker probe in the brain tissue was further analyzed by NIH ImageJ (Online Resource 6). Thus, our method for assessing the mitochondrial membrane potential of brain and striatal neurons in vivo may contribute to understanding the mitochondrial dysfunction in HD animals. Additionally, we evaluated the ultrastructural change of the mitochondria and synapse in the striatal neurons of R6/2 mouse with and without NDGA administration. The mitochondrial membrane and cristae structure was deformed in the striatal neuron of R6/2 mice in comparison to the mitochondria of control mice (Fig. 6b). NDGA treatment restored the ultrastructural morphology of mitochondria in R6/2 mice. These electron microscopic data support the fact that NDGA prevents neuronal mitochondria damage in vitro (Fig. 5c) and in vivo (Fig. 6b). The synapse morphology in the striatum of

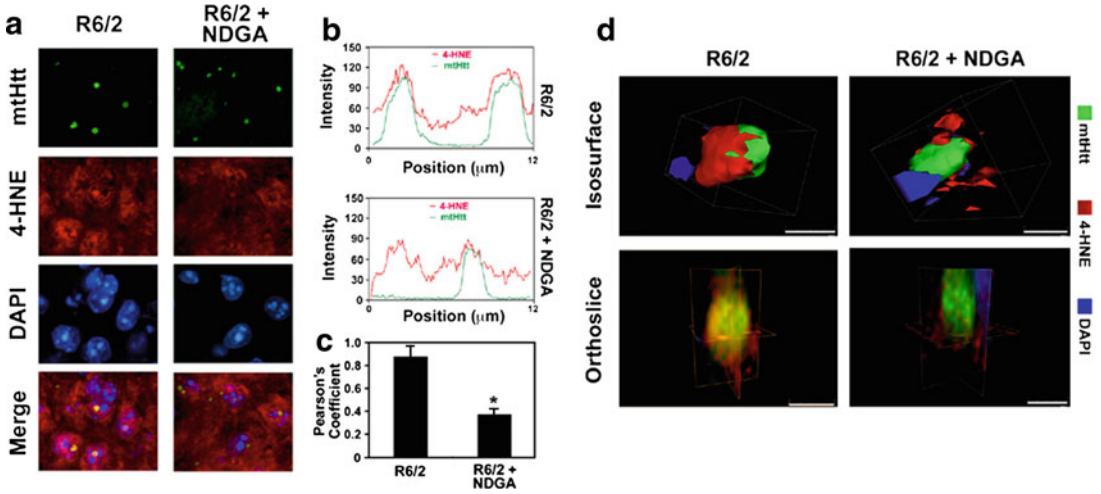

Fig. 5 Analysis for the colocalization of 4-HNE adducts with mtHtt using deconvolved and 3D constructed confocal images. **a** Deconvolved isosurface images show structures of 4-HNE adducts (*red*) and mtHtt (*green*) in the striatal neuron of R6/2 mice. NDGA reduces the level of 4-HNE and mtHtt and separate the spatial distribution of two molecules. Deconvolved orthoslice images confirm that NDGA decreases the colocalization of 4-HNE and mtHtt. **b** The reduction of 4-HNE and mtHtt intensity by NDGA administration in R6/2 mice. The intensity of 4-HNE (*green*) and mtHtt (*red*) were measured by the line measurement (AQI-X-COMBO-CWF, Media cybernetics Inc. Bethesda, MD, USA). **c** NDGA reduces the colocalization of 4-HNE and mtHtt nuclear structure. Images taken from three fields were analyzed. *Significantly different vehicle-treated R6/2 mice at $P < 0.01$. **d** Analysis for the colocalization of 4-HNE adducts with mtHtt using deconvolved and 3D constructed confocal images. Deconvolved isosurface images show structures of 4-HNE adducts (*red*) and mtHtt (*green*) in the striatal neuron of R6/2 mice. NDGA reduces the level of 4-HNE and mtHtt and separate the spatial distribution of two molecules. Deconvolved orthoslice images confirm that NDGA decreases the colocalization of 4-HNE and mtHtt. *Scale bars* 15 μm

NDGA-administered R6/2 mice shows improvement with structure similar to the control mice (Fig. 6c).

NDGA improves gross brain neuropathology and extends the survival of HD (R6/2) transgenic mice

To determine if NDGA plays a role in preventing the neuropathology and extending the survival in an animal model of HD, we examined the in vivo effect of NDGA in R6/2 mice. NDGA (12 mg/kg/day) was administered from 30 days of age to 90 days of age. Serial-cut coronal tissue sections revealed gross brain atrophy and flattening of the medial aspect of the striatum in the R6/2 brains compared with WT brains (Fig. 7a). NDGA ameliorated these gross neuropathological sequelae in R6/2 mice compared with vehicle-treated mice at 3 months of age (Fig. 7a). The atrophy of striatal neuron was markedly present in R6/2 mice (Fig. 7a). Indeed, striatal neuronal size was significantly improved in NDGA-treated mice (93.01 ± 2.48 μm^2) ($F_{(3,22)} = 4.60$; $P < 0.05$) that are similar to WT littermate control (100.63 ± 2.80 μm^2), comparing with vehicle-treated R6/2 (64.35 ± 5.23 μm^2) ($F_{(3,22)} = 3.42$; $P < 0.01$) mice (Fig. 7b). The overall improvements of neuropathology were coincident with survival extension by 19% (vehicle-treated R6/2, 105 days; NDGA-treated R6/2, 125 days; $\chi^2 = 9.23$; $P < 0.01$) (Fig. 7c). The body weight of R6/2 mice dropped significantly at 105 days of age, but NDGA restored body weight significantly ($F_{(4,60)} = 7.910$; $P < 0.01$) (Fig. 7d).

Discussion

Oxidative damage has been implicated in the pathogenesis of neuronal degeneration in a wide range of disorders, and membrane lipids in particular are a major target of reactive oxygen species (ROS). We showed that therapy with NDGA, which reduces lipid peroxidation and mitochondrial dysfunction, reduces the pathological phenotype in HD mice. NDGA is a lignan found in the leaves and twigs of the shrub *Larrea tridentate* [2]. It has antioxidant activity and is used commercially as a food additive to preserve fats and butter. NDGA has recently been found to activate estrogen receptor (ER)-mediated actions and to possess a specific ER modulator-like activity, preferentially inducing ER alpha-mediated transcription while showing mixed agonism/antagonism of ER beta-mediated transcription in an estrogen-responsive cell line [10]. Lignan-type phytoestrogens bind to ERs with very low affinity, and high concentrations are required to manifest ER-mediated actions. In our study, we confirmed that the neuroprotective effect of NDGA is not dependent on transcriptional activation of ER in primary neurons (Online Resource 7). NDGA is also a selective inhibitor of 12-lipoxygenase

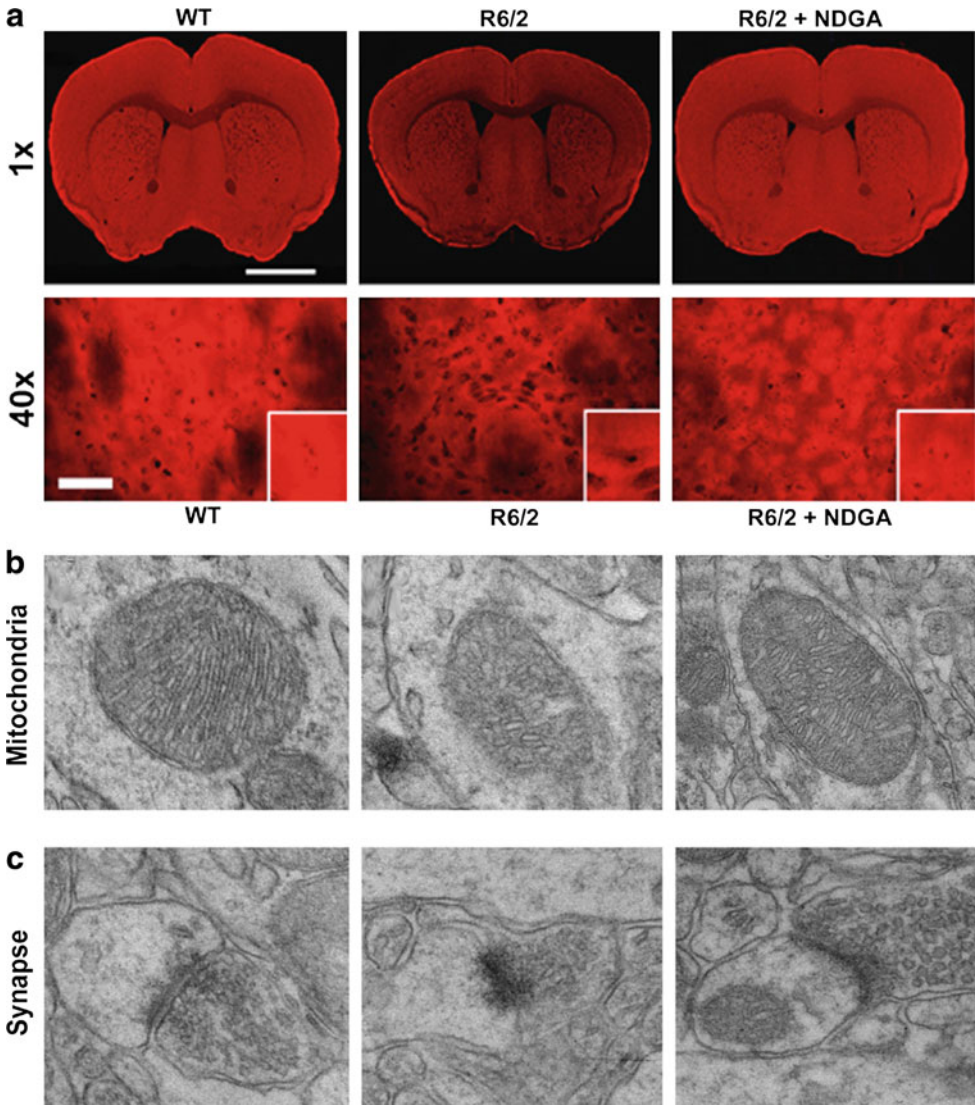

Fig. 6 NDGA restores the mitochondrial membrane potential and improves the ultrastructure of mitochondria and synapse in striatal neurons of R6/2 mice. **a** Enhancement of mitochondrial membrane potential by NDGA in HD (R6/2) transgenic mice. Fluorescent photomicrographs of striatal sections stained with CMXRos (*red*). NDGA treatment was started in 6-week-old mice for 3 weeks. CMXRos (100 nM) was injected i.p. 48 h before the perfusion of mice. *Scale bars* 1× 2 mm; 40× 50 μm. **b** NDGA treatment improves the ultrastructure of mitochondria in the striatal neurons of R6/2 mouse. **c** NDGA improves the morphology of synapse in the striatum of R6/2 mice which is similar to the control mice. Ultrastructural change of the mitochondria and synapse in the striatum of R6/2 mouse was found by TEM

(12-LOX), which produces ROS during arachidonic acid metabolism [20]. Activation of 12-LOX is produced by glutamate cytotoxicity and glutathione depletion. Because a number of eicosanoid metabolites generated by 12-LOX play critical roles in the induction of the neuronal cell death via oxidative stress, inhibition of 12-LOX activity promotes neuronal cell survival [18]. In order to determine whether the neuroprotective effect of NDGA is mediated by 12-LOX inhibition, we tested the effect of 12-HETE, a byproduct of 12-LOX, on neuronal viability against oxidative stress. We surmised that if NDGA's neuroprotection is related to the 12-LOX pathway, then 12-HETE should enhance its pro-apoptotic effects under oxidative stress. Our data demonstrated, however, that 12-HETE protects neurons from oxidative stress suggesting that the neuroprotective effect of NDGA is most likely an off target effect not related to 12-LOX inhibition (Online Resource 8). A number of other biochemical pathways could be responsible for the neuroprotective effect of NDGA, and the exact mechanism remains to be defined [40]. Our present data also suggest that NDGA's neuroprotective effect may be due to reduced lipid peroxidation and improved mitochondrial function [11]. Mitochondrial membrane potential is an important subcellular marker for monitor oxidative stress signals related to neuronal cell survival and death [25]. The mitochondrion is one of the major targets for free radical-mediated damage, but its role as a contributor to oxidative stress is HD is controversial. Lee et al. [16] report that the polyQ modulates huntingtin's role in extra-mitochondrial energy metabolism rather than by directly impacting mitochondria in STHdh(Q111/Q111) cells, an HD knock-in model. Furthermore, mitochondrial function does not appear to be altered at early stages in other two knock-in mice models [19, 28]. Therapeutic strategies targeting mitochondria-dependent pathways will require further study to more fully understand mechanisms

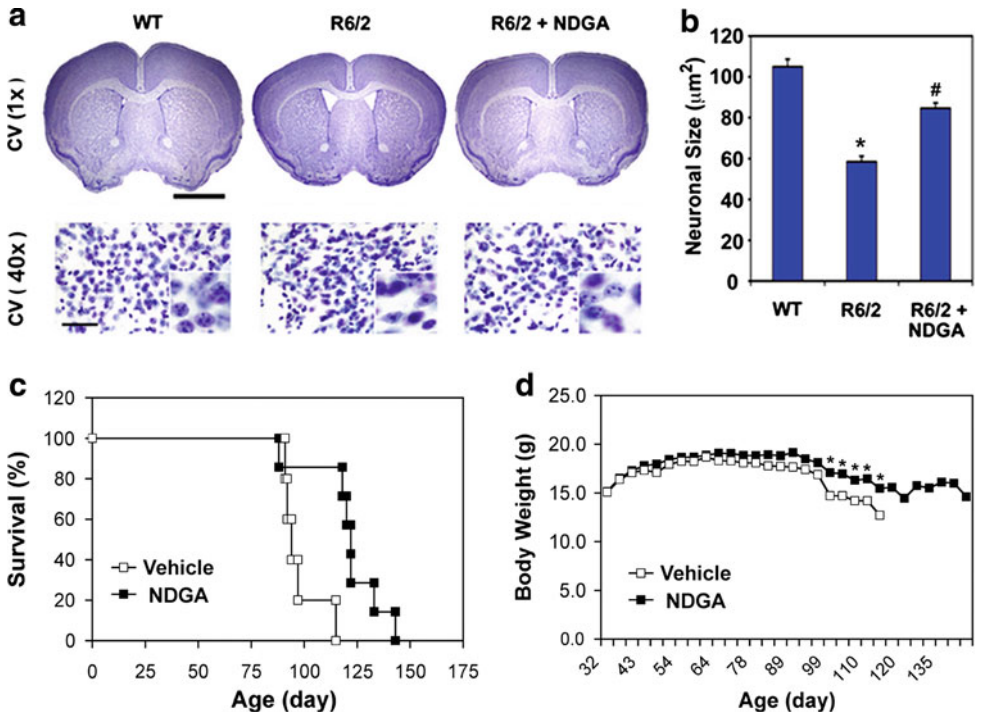

Fig. 7 NDGA improves gross brain and histopathological sequelae and extends the survival of R6/2 mice. **a** Photomicrographs of coronal sections from the rostral neostriatum at the level of the anterior commissure in a wild-type littermate mouse, a vehicle-treated R6/2 mouse, and a NDGA-treated R6/2 mouse. Corresponding Nissl-stained tissue sections from the dorsomedial aspect of the neostriatum in a wild-type littermate control, vehicle-treated R6/2 mouse, and NDGA-treated R6/2 mouse are also shown. *Scale bars* 1× 2 mm; 40× 100 μm. **b** NDGA ameliorates neuronal atrophy and improves neuronal size. Five animals per group were used for neuronal size analysis. Data were analyzed by ANOVA. *Significantly different from control, $P < 0.01$; #significantly different from vehicle-treated R6/2 mouse, $P < 0.05$. **c** Kaplan–Meier probability of survival analysis of NDGA treatment in R6/2 mice ($n = 10$) and vehicle-treated R6/2 mice ($n = 10$). **d** Effect of NDGA treatment on body weight in R6/2 mice. *Significantly different from vehicle-treated R6/2 mouse, $P < 0.01$

of energy failure and to develop appropriate treatments in HD.

The 4-HNE is relatively more stable than free radicals and passes easily among subcellular compartment to react with a variety of biomolecules bearing thiol and amino groups [38]. Previous research showed that the α-synuclein associates with 4-HNE to generate protein adducts that could serve as biomarkers in cellular models of α-synuclein aggregation and pathology [43]. In addition, 4-HNE, presumably resulting from the peroxidation of lipids, is increased in Alzheimer's disease (AD) patients and is found in amyloid beta peptide (Abeta) plaques associated with AD [40]. 4-HNE covalently modifies Abeta, triggering its aggregation. As a consequence, 4-HNE accelerates the formation of Abeta protofibrils while inhibiting the production of straight, mature fibrils [42]. Recent studies implicating Abeta oligomers and protofibrils in the neurotoxic process that ultimately leads to AD suggest that the Abeta aggregates induced by 4-HNE may be relevant to the pathogenesis of AD [31, 42]. In addition, 4-HNE deposits are found in the brains of patients with myotonic dystrophy [26], and 4-HNE levels are elevated in the cerebrospinal fluid of patients with amyotrophic lateral sclerosis (ALS) [48].

Our research indicates that increased 4-HNE deposition is a marker of the excessive lipid peroxidation in HD. Our data indicate that oxidative events are responsible for increased 4-HNE levels and mtHtt inclusion formation in a cellular model of HD. Interestingly, we found that 4-HNE adducts immunoreactivity was distributed in nuclear foci that is spatially colocalized with mtHtt in striatal neurons of the R6/2 mice. In contrast, there was no significant alteration in the level of malondialdehyde (MDA) adducts, another lipid peroxidation marker, in the striatum of HD mice (Online Resource 9). Modifications of mtHtt produced by 4-HNE could substantially alter its physical properties as well as increase its toxicity and contribute to inclusion body formation.

While there are no present treatments to ameliorate or arrest the neuropathological alterations in HD patients, significant advances have been made in animal models of HD [47]. These advancements have recently initiated a number of clinical trials [20, 26, 36]. We explored whether therapeutic modulation of oxidative stress and

mitochondrial function by NDGA affects 4-HNE levels or mtHtt aggregation in R6/2 HD mice. As we expected, NDGA decreased the level of 4-HNE adducts in striatal neurons of R6/2 mice. In addition, the colocalization of 4-HNE adducts with mtHtt were reduced by NDGA, while the majority of 4-HNE immunoreactivity was spatially merged to the prominent clusters of mtHtt in vehicle-treated R6/2 mice. It is most likely that the decrease of mtHtt inclusions is correlated with the reduction of 4-HNE adducts by NDGA administration raising the possibility that NDGA may directly inhibit aggregation of mtHtt consistent with previous findings regarding the anti-fibrillogenic and fibril-destabilizing effects of NDGA on Abeta aggregation and α-synuclein fibrils [13, 26, 27].

Our data indicate that the increased level of 4-HNE adducts, identified in both human and animal models of HD, is a useful molecular marker for the oxidative damage in HD. We have determined that indications of oxidative stress elevate the level of 4-HNE adducts and mtHtt inclusions in HD and believe that the lipid peroxidation pathway may be a novel therapeutic target for preventing known oxidative injury in HD. It remains evident that further mechanistic and detailed studies will be of enormous value to further understand the role of 4-HNE on mtHtt modifications.

The administration of NDGA resulted in a beneficial effect in neurons by modulating the mitochondrial function and oxidative stress. In addition, NDGA ameliorated the neuropathology and extended the survival of R6/2 transgenic HD mice [41]. Our findings suggest that NDGA may be a candidate for future clinical trials in HD and other neurodegenerative disorders.

Acknowledgments We thank to Katharine Karr and Yu Jin Hwang for the preparation of manuscript. This study was supported by NIH NS52724 (H.R.).

References

1. Albers DS, Beal MF (2000) Mitochondrial dysfunction and oxidative stress in aging and neurodegenerative disease. J Neural Transm Suppl 59:131–154
2. Arteaga S, Andrade-Cetto A, Cárdenas R (2005) *Larrea tridentata* (Creosote bush), an abundant plant of Mexican and US-American deserts and its metabolite nordihydroguaiaretic acid. J Ethnopharmacol 98:231–239
3. Beal MF (1995) Aging, energy and oxidative stress in neurodegenerative diseases. Ann Neurol 38:357–366
4. Beal MF, Ferrante RJ (2004) Experimental therapeutics in transgenic mouse models of Huntington's disease. Nat Rev Neurosci 5:373–384
5. Bosco DA, Fowler DM, Zhang Q, Nieva J, Powers ET, Wentworth P Jr et al (2006) Elevated levels of oxidized cholesterol metabolites in Lewy body disease brains accelerate alpha-synuclein fibrilization. Nat Chem Biol 2:249–253
6. Browne SE, Beal MF (2006) Oxidative damage in Huntington's disease pathogenesis. Antioxid Redox Signal 8:2061–2073
7. Comporti M (1998) Lipid peroxidation and biogenic aldehydes: from the identification of 4-hydroxynonenal to further achievements in biopathology. Free Radic Res 28:623–635
8. Ferrante RJ, Kubilus JK, Lee J, Ryu H, Beesen A, Zucker B et al (2003) Histone deacetylase inhibition by sodium butyrate chemotherapy ameliorates the neurodegenerative phenotype in Huntington's disease mice. J Neurosci 23:9418–9427
9. Fischbeck KH (2001) Polyglutamine expansion neurodegenerative disease. Brain Res Bull 56:161–163
10. Fujimoto N, Kohta R, Kitamura S, Honda H (2004) Estrogenic activity of an antioxidant, nor dihydroguaiaretic acid (NDGA). Life Sci 74:1417–1425
11. Goodman Y, Steiner MR, Steiner SM, Mattson MP (1994) Nordihydroguaiaretic acid protects hippocampal neurons against amyloid beta-peptide toxicity, and attenuates free radical and calcium accumulation. Brain Res 654:171–176
12. Hall ED, Andrus PK, Oostveen JA, Fleck TJ, Gurney ME (1998) Relationship of oxygen radical-induced lipid peroxidative damage to disease onset and progression in a transgenic model of familial ALS. J Neurosci Res 53:66–77
13. Hamaguchi T, Ono K, Murase A, Yamada M (2009) Phenolic compounds prevent Alzheimer's pathology through different effects on the amyloid-beta aggregation pathway. Am J Pathol 175:2557–2565
14. Hersch SM, Ferrante RJ (1997) Neuropathology and pathophysiology of Huntington's disease. In: Watts RL, Koller WC (eds) Movement disorders: neurologic principles and practice. McGraw-Hill, New York, pp 503–518
15. Huntington's Disease Collaborative Research Group (1993) A novel gene containing a trinucleotide repeat that is expanded and unstable on Huntington's disease chromosomes. Cell 72:971–983
16. Lee JM, Ivanova EV, Seong IS, Cashorali T, Kohane I, Gusella JF, MacDonald ME (2007) Unbiased gene expression analysis implicates the huntingtin polyglutamine tract in extra-mitochondrial energy metabolism. PLoS Genet 3:e135
17. Levine MS, Klapstein GJ, Koppel A, Gruen E, Cepeda C, Vargas ME et al (1999) Enhanced sensitivity to *N*-methyl-D-aspartate receptor activation in transgenic and knockin mouse models of Huntington's disease. J Neurosci Res 58:515–532
18. Li Y, Maher P, Schubert D (1997) A role for 12-lipoxygenase in nerve cell death caused by glutathione depletion. Neuron 19:453–463
19. Li X, Sapp E, Chase K, Comer-Tierney LA, Masso N, Alexander J, Reeves P, Kegel KB, Valencia A, Esteves M, Aronin N, Difiglia M (2009) Disruption of Rab11 activity in a knock-in mouse model of Huntington's disease. Neurobiol Dis 36:374–383
20. Mangiarini L, Sathasivam K, Seller M, Cozens B, Harper A, Hetherington C, Lawton M, Trottier Y, Lehrach H, Davies SW, Bates GP (1996) Exon 1 of the HD gene with an expanded CAG repeat is sufficient to cause a progressive neurological phenotype in transgenic mice. Cell 87:493–506
21. McGrath LT, McGleenon BM, Brennan S, McColl D, McILroy S, Passmore AP (2001) Increased oxidative stress in Alzheimer's disease as assessed with 4-hydroxynonenal but not malondialdehyde. QJM 94:485–490
22. Montine TJ, Neely MD, Quinn JF, Beal MF, Markesbery WR, Roberts LJ et al (2002) Lipid peroxidation in aging brain and Alzheimer's disease. Free Radic Biol Med 33:620–626
23. Neely MD, Sidell KR, Graham DG, Montine TJ (1999) The lipid peroxidation product 4-hydroxynonenal inhibits neurite outgrowth, disrupts neuronal microtubules, and modifies cellular tubulin. J Neurochem 72:2323–2333
24. Neely MD, Boutte A, Milatovic D, Montine TJ (2005) Mechanisms of 4-hydroxynonenal-induced neuronal microtubule dysfunction. Brain Res 1037:90–98

25. Nicholls DG, Ward MW (2000) Mitochondrial membrane potential and neuronal glutamate excitotoxicity: mortality and millivolts. Trends Neurosci 23:166–174
26. Ono K, Hasegawa K, Yoshiike Y, Takashima A, Yamada M, Naiki H (2002) Nordihydroguaiaretic acid potently breaks down pre-formed Alzheimer's beta-amyloid fibrils in vitro. J Neurochem 81:434–440
27. Ono K, Yamada M (2006) Antioxidant compounds have potent anti-fibrillogenic and fibril-destabilizing effects for alpha-synuclein fibrils in vitro. J Neurochem 97:105–115
28. Orr AL, Li S, Wang CE, Li H, Wang J, Rong J, Xu X, Mastroberardino PG, Greenamyre JT, Li XJ (2008) N-terminal mutant huntingtin associates with mitochondria and impairs mitochondrial trafficking. J Neurosci 28:2783–2792
29. Oyamada R, Hayashi M, Katoh Y, Tsuchiya K, Mizutani T, Tominaga I et al (2006) Neurofibrillary tangles and deposition of oxidative products in the brain in cases of myotonic dystrophy. Neuropathology 26:107–114
30. Panov AV, Gutekunst CA, Leavitt BR, Hayden MR, Burke JR, Strittmatter WJ et al (2002) Early mitochondrial calcium defects in Huntington's disease are a direct effect of polyglutamines. Nat Neurosci 5:731–736
31. Qahwash IM, Boire A, Lanning J, Krausz T, Pytel P, Meredith SC (2007) Site-specific effects of peptide lipidation on beta-amyloid aggregation and cytotoxicity. J Biol Chem 282:36987–36997
32. Ratan RR, Ryu H, Lee J, Mwidau A, Neve RL (2002) In vitro model of oxidative stress in cortical neurons. Methods Enzymol 352:183–190
33. Ryu H, Lee J, Olofsson BA, Mwidau A, Dedeoglu A, Escudero M et al (2003) Histone deacetylase inhibitors prevent oxidative neuronal death independent of expanded polyglutamine repeats via an SP1-dependent pathway. Proc Natl Acad Sci USA 100:4281–4286
34. Ryu H, Lee J, Zaman K, Kubilis J, Ferrante RJ, Ross BD et al (2003) SP1 and SP3 are oxidative stress-inducible, anti-death transcription factors in cortical neurons. J Neurosci 23:3597–3606
35. Ryu H, Ferrante RJ (2005) Emerging chemotherapeutic strategies for Huntington's disease. Expert Opin Emerg Drugs 10:345–363
36. Ryu H, Lee J, Hagerty SW, Soh BY, McAlpin SE, Cormier KA et al (2006) ESET/SETDB1 gene expression and histone H3 (K9) trimethylation in Huntington's disease. Proc Natl Acad Sci USA 103:19176–19181
37. Sawa A, Wiegand GW, Cooper J, Margolis RL, Sharp AH, Lawler JF Jr et al (1999) Increased apoptosis of Huntington disease lymphoblasts associated with repeat length-dependent mitochondrial depolarization. Nat Med 5:1194–1198
38. Schaur RJ (2003) Basic aspects of the biochemical reactivity of 4-hydroxynonenal. Mol Aspects Med 24:149–159
39. Schilling G, Becher MW, Sharp AH, Jinnah HA, Duan K, Kotzuk JA et al (1999) Intranuclear inclusions and neuritic aggregates in transgenic mice expressing a mutant N-terminal fragment of huntingtin. Hum Mol Genet 8:397–407
40. Sexton A, McDonald M, Cayla C, Thiemermann C, Ahluwalia A (2007) 12-Lipoxygenase-derived eicosanoids protect against myocardial ischemia/reperfusion injury via activation of neuronal TRPV1. FASEB J 21:2695–2703
41. Shishido Y, Furushiro M, Hashimoto S, Yokokura T (2001) Effect of nordihydroguaiaretic acid on behavioral impairment and neuronal cell death after forebrain ischemia. Pharmacol Biochem Behav 69:469–474
42. Siegel SJ, Bieschke J, Powers ET, Kelly JW (2007) The oxidative stress metabolite 4 hydroxynonenal promotes Alzheimer protofibril formation. Biochemistry 46:1503–1510
43. Trostchansky A, Lind S, Hodara R, Oe T, Blair IA, Ischiropoulos H et al (2006) Interaction with phospholipids modulates alpha-synuclein nitration and lipid-protein adduct formation. Biochem J 393:343–349
44. Truant R, Atwal RS, Burtnik A (2007) Nucleocytoplasmic trafficking and transcription effects of huntingtin in Huntington's disease. Prog Neurobiol 83:211–227
45. Trushina E, McMurray CT (2007) Oxidative stress and mitochondrial dysfunction in neurodegenerative diseases. Neuroscience 145:1233–1248
46. Vonsattel JP, Myers RH, Stevens TJ, Ferrante RJ, Bird ED, Richardson EP Jr (1985) Neuropathological classification of Huntington's disease. J Neuropathol Exp Neurol 44:559–577
47. Vonsattel JP (2008) Huntington disease models and human neuropathology: similarities and differences. Acta Neuropathol 115:55–69
48. Zarkovic K (2003) 4-Hydroxynonenal and neurodegenerative diseases. Mol Aspects Med 24:293–303